Combustion Theory and Modelling, 2013
Vol. 17, No. 6, 983–1002, http://dx.doi.org/10.1080/13647830.2013.818717

Triple-flame propagation against a Poiseuille flow in a channel with porous walls

Faisal Al-Malki[a] and Joel Daou[b*]

[a]*Department of Mathematics, Taif UniversityTaif P.O. Box 888, Saudi Arabia;* [b]*School of Mathematics, University of Manchester, Manchester M13 9PL, UK*

(*Received 4 March 2013; accepted 13 June 2013*)

We present an essentially numerical study of triple-flame propagation in a non-strained two-dimensional mixing layer against a Poiseuille flow, within a thermo-diffusive model. The aim of the study is twofold. First, to examine the recent analytical findings derived in the asymptotic limit of infinite Zeldovich number β for flame fronts thin compared with their typical radius of curvature and to extend these to finite-values of β. Second, to gain insight into the influence of the flow on the flame in situations where the flame in not necessarily thin, as assumed analytically. The study has focused on the effect of two main non-dimensional parameters on flame propagation, namely the flow amplitude A and the flame-front thickness ϵ. For moderate values of A, the flow is found to have a negligible effect on the structure of the flame, while modifying its speed by an amount proportional to A, in agreement with the asymptotic findings. Two new qualitative behaviours are found however. The first is obtained for sufficiently large values of A where the flow is shown to modify the flame structure significantly for small values of ϵ; more precisely, the concavity of the triple-flame front is found to turn towards the unburnt gas for A larger than a critical value. This inversion of the front curvature, which cannot be captured by the infinitely-large β asymptotic study, is found to be intimately linked to the finite values of β, which are necessarily found in any realistic model or computational study. The second new behaviour, which is also obtained for small ϵ, is the existence of termination-points on the flame front, or flame-tips. These termination-points are shown to exist for $\epsilon \ll 1$ only if A takes on positive values of order unity or larger; in particular they are absent for thin triple-flames without the presence of a non-uniform flow field. Furthermore, several additional novel contributions are made in the present context of triple-flame interaction with a non-uniform parallel flow. These include a fairly complete description of the flame propagation regimes for a wide range of variations in A and ϵ. In particular, it is found that larger values of A promote combustion by increasing the ϵ-range of existence of ignition fronts, while a decrease in the value of A towards zero or negative values increases the ϵ-range of existence of extinction fronts.

Keywords: Triple-flames; flame–flow interaction; partially premixed flames; Poiseuille flow; porous-walls channel

1. Introduction

Triple-flames are one of the fundamental structures in combustion which can be observed in a wide range of applications involving phenomena such as flame propagation in mixing layers, flame spread over solid fuel surfaces and autoignition fronts in diesel engines [1]. These structures, consisting of two premixed branches and a trailing diffusion flame, appear

*Corresponding author. Email: joel.daou@manchester.ac.uk

in situations where the reactive mixture itself involves composition inhomogeneities such as those in the mixing layers of initially non-premixed reactants. Typically, the composition of the mixture varies across the mixing layer from fuel-lean to fuel-rich conditions, which upon successful ignition leads to the formation of triple-flames. A considerable research effort has been devoted to the study of triple-flames both experimentally [2] and theoretically [3, 4]. Theoretically, in particular, many factors influencing the propagation of triple-flames have been examined such as the transverse composition gradient [3, 5], preferential diffusion [6], heat losses [7, 8, 9], variable density [10] and many others [11, 12, 13, 14], which we do not review here.

In a recent study [15], the present authors have investigated analytically the effect of a parallel flow on triple-flame propagation. For the sake of tractability, and also to concentrate on the coupling between the non-uniform flow field and thermo-diffusive effects, this study has adopted the constant density approximation. This has permitted an asymptotic analysis to be carried out in the limit of infinitely large activation energy and restricted to thin flames. The analysis has described the influence of the flow in terms of two main non-dimensional parameters, the flow amplitude and its scale. It has been shown in particular that for large scale flows, such as the Poiseuille flow considered in this paper, the flow negligibly affects the flame structure except for a change in its speed by an amount which depends on the stoichiometric conditions of the mixture. In particular, analytical expressions describing the flame characteristics such as the location of its leading edge, its propagation speed and its curvature have been obtained. One of the aims of the present numerical study is to assess the validity of the asymptotic findings in [15]. Another aim is to extend the analysis, by examining the flame behaviour outside the range of validity of the asymptotics which preclude important features such as the occurrence of extinction fronts. Finally, the investigation aims at providing useful insight extracted from a simple model which can motivate further work related to the interaction between a non-uniform flow field and a flame propagating in a non-uniform reactive mixture; indeed, dedicated studies in such a field of investigation seem to be rare, at least from the theoretical point of view. Following this work, which as we shall see will reveal several new behaviours summarised in the abstract, important realistic effects such as variable density and heat losses can be incorporated in the model for future investigation.

The paper is structured as follows. The thermo-diffusive model adopted is described in Section 2. This is followed by a summary of a few useful analytical results from the recent analytical study [15]; these are essential for proper understanding of the work and are used for interpreting the results. Specifically, formulas are given for the local burning speed and propagation velocity of the triple-flame in cases where the thickness of the flame front relative to its typical radius of curvature, measured by a non-dimensional parameter ϵ, is small. These formulas are, in principle, applicable for situations where the scale of the flow (measured with the radius of curvature) is of order unity, or larger. The numerical study along with its main results are presented in Section 4 followed by concluding remarks and a summary of the main findings in Section 5.

2. Formulation

The problem considered here is triple-flame propagation in a channel of width $2L$ against a Poiseuille flow along the X-direction, as shown in Figure 1. It is assumed that the walls of the channel are porous and that the concentrations of fuel and oxidiser are maintained fixed there. A detailed formulation of the problem has been given in [15], which can be

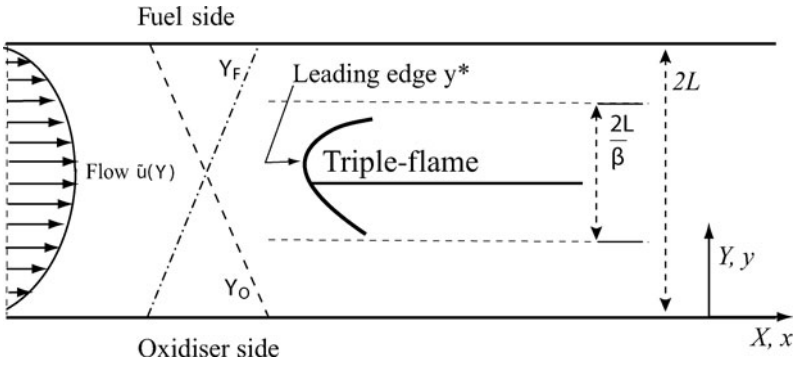

Figure 1. A triple-flame propagating against a Poiseuille flow $\tilde{u}(Y) = \tilde{A}[1 - (Y^2/L^2)]$ in a channel of width $2L$. The mass fractions are prescribed by $Y_F = Y_{F,F}$ and $Y_O = 0$ on the fuel side, and $Y_F = 0$ and $Y_O = Y_{O,O}$ on the oxidiser side, with $T = T_u$ on both sides. The upstream (far to the left) boundary conditions correspond to frozen profiles, varying linearly with Y between the wall values.

consulted for further details, if needed. Here, our aim is to present the final thermo-diffusive non-dimensional model along with the necessary notation. The combustion is represented by a single irreversible one-step reaction of the form

$$\mathrm{F} + s\mathrm{O} \rightarrow (1+s)\mathrm{P} + q,$$

where F denotes the fuel, O the oxidiser and P the products. The quantities s and q represent the mass of oxidiser consumed and the heat released, both per unit mass of fuel. The reaction rate $\tilde{\omega}$, defined as the mass of fuel consumed per unit volume and unit time, is assumed to follow an Arrhenius law

$$\tilde{\omega} = B\rho^2 Y_F Y_O \exp(-E/RT),$$

where ρ is the (constant) density, B the pre-exponential factor, E the activation energy, and R the universal gas constant. Here T, Y_F and Y_O represent the temperature and the mass fractions of the fuel and oxidiser, respectively.

For large activation energies, the flame-front region is expected to be centred around the stoichiometric surface where $Y_O = sY_F$. Upstream, the frozen profiles being linear, this surface is located at $Y = Y_{st}$ given by

$$\frac{Y_{st}}{L} = \frac{1-S}{1+S},$$

where $S \equiv sY_{F,F}/Y_{O,O}$ is a normalised stoichiometric coefficient. Using the subscript 'st' to indicate values at ($X \rightarrow -\infty$, $Y = Y_{st}$), we introduce the scaled quantities

$$y_F = \frac{Y_F}{Y_{F,st}}, \quad y_O = \frac{Y_O}{Y_{O,st}}, \quad \theta = \frac{T - T_u}{T_{ad} - T_u},$$

where $T_{ad} \equiv T_u + qY_{F,st}/c_p$ is the adiabatic flame temperature.

For non-dimensionalisation, we select as unit length L/β, the ratio between the mixing layer thickness and the Zeldovich number $\beta \equiv E(T_{\rm ad} - T_u)/RT_{\rm ad}^2$ and as unit speed the laminar speed of the stoichiometric planar flame S_L^0, which for large β is given by

$$S_L^0 = \frac{4{\rm Le_F Le_O}}{\beta^3} Y_{\rm Ost}(\rho D_T) B \exp(-E/RT_{\rm ad}),$$

where D_T is the thermal diffusivity, and $\rm Le_F$ and $\rm Le_O$ are respectively the fuel and oxidiser Lewis numbers.

The non-dimensional governing equations in a frame of reference attached to the flame front are

$$(V + u(y))\frac{\partial \theta}{\partial x} = \epsilon \left(\frac{\partial^2 \theta}{\partial x^2} + \frac{\partial^2 \theta}{\partial y^2} \right) + \epsilon^{-1} \omega \tag{1}$$

$$(V + u(y))\frac{\partial y_{\rm F}}{\partial x} = \frac{\epsilon}{{\rm Le_F}} \left(\frac{\partial^2 y_{\rm F}}{\partial x^2} + \frac{\partial^2 y_{\rm F}}{\partial y^2} \right) - \epsilon^{-1} \omega \tag{2}$$

$$(V + u(y))\frac{\partial y_{\rm O}}{\partial x} = \frac{\epsilon}{{\rm Le_O}} \left(\frac{\partial^2 y_{\rm O}}{\partial x^2} + \frac{\partial^2 y_{\rm O}}{\partial y^2} \right) - \epsilon^{-1} \omega, \tag{3}$$

when written in terms of the coordinates $x = \beta X/L$ and $y = \beta(Y - Y_{\rm st})/L$. Here

$$\epsilon \equiv \frac{\ell_{\rm Fl}}{L/\beta} = \frac{D_T/S_L^0}{L/\beta} \tag{4}$$

represents the thickness of the laminar stoichiometric flame $\ell_{\rm Fl} \equiv D_T/S_L^0$ measured with the reference length L/β. The terms V and $u(y)$ denote the non-dimensional propagation speed and flow velocity in the laboratory frame of reference, with $V > 0$ indicating propagation to the left. In fact, $u(y)$ has the form

$$u(y) = A \left(1 - \left\{ \frac{1 - S}{1 + S} + \frac{y}{\beta} \right\}^2 \right), \tag{5}$$

which corresponds to the dimensional form of the Poiseuille flow $\tilde{u}(Y) = \tilde{A}[1 - (Y^2 L^2)]$ with $A = \tilde{A}/S_L^0$. Finally, the reaction rate ω is given by

$$\omega = \frac{\beta^3}{4{\rm Le_F Le_O}} y_{\rm F} y_{\rm O} \exp\left[\frac{\beta(\theta - 1)}{1 + \alpha(\theta - 1)} \right],$$

where $\alpha = (T_{\rm ad} - T_u)/T_{\rm ad}$.

The upstream and lateral boundary conditions are

$$\theta = 0 \tag{6a}$$

$$y_{\rm F} = 1 + \frac{(1 + S)y}{2\beta} \tag{6b}$$

$$y_{\rm O} = 1 - \frac{(1 + S)y}{2\beta S}, \qquad \text{as} \quad x \to -\infty,\ y \to \frac{2\beta S}{1 + S} \ \text{ or } \ y \to -\frac{2\beta}{1 + S}. \tag{6c}$$

Downstream, we require that

$$\frac{\partial y_F}{\partial x} = \frac{\partial y_O}{\partial x} = \frac{\partial \theta}{\partial x} = 0 \qquad \text{as } x \to \infty. \tag{7}$$

The problem formulation is now complete, and is given by Equations (1)–(3) with the boundary conditions (6)–(7). The solution of this problem can provide, in addition to the profiles of θ, y_F and y_O, the flame speed V in terms of ϵ, A, β, S, $\mathrm{Le_F}$, $\mathrm{Le_O}$ and α.

As mentioned earlier, an analytical description of the problem is possible under a suitably defined distinguished asymptotic limit, which is presented in [15] and briefly summarised in the following section. The approach of this paper is numerical, however. One focus of the numerical study is on examining the validity of the asymptotic findings, and in fact to show that these are not necessarily valid in common situations when the activation energy if finite. Another main focus is on describing the influence of the flow outside the range of applicability of the asymptotic analysis, and constitute an essential addition to our previous work so as fully to describe the influence of a Poiseuille flow on a triple-flame.

3. Essential asymptotic results

We have carried out in [15] an asymptotic analysis of the problem above, valid for large values of β and small values of ϵ (with $\beta^{-1} \ll \epsilon$). The methodology follows that used in the strained-mixing layer [6]. The reaction zone is modelled as an infinitely thin sheet (given by $x = f(y)$ say) across which jump conditions are applicable in the limit $\beta \to \infty$ with the parameters $l_F \equiv \beta(\mathrm{Le_F} - 1)$ and $l_O \equiv \beta(\mathrm{Le_O} - 1)$ being of order one.

We shall state here the main result of [15] which is relevant to the present investigation as a two-term expansion in ϵ for the flame speed V, namely

$$V \sim S_{Lo}(y^*) - u(y^*) - \epsilon f_0''(y^*)\left[1 + \frac{l_F + l_O}{2} - \frac{l_F - l_O}{2}\frac{(S+1)^2 y^*}{4S + (S+1)^2|y^*|}\right]. \tag{8}$$

Here $S_{Lo}(y)$, $f_0(y)$, and y^* represent the local burning speed, the flame-front shape and the location of the leading edge, to leading order. For S_{Lo}, we have the explicit expression

$$S_{Lo}(y) = \sqrt{1 + \frac{(S+1)^2}{4S}|y|}\ \exp\left(\frac{(S^2-1)y - (S+1)^2|y|}{8S}\right), \tag{9}$$

which shows its dependence on the transverse coordinate y and the stoichiometric coefficient S. As for the leading edge y^*, which need not be unique, we show that it must correspond to a maximum of $S_{Lo}(y) - u(y)$, which can be worked out if the flow is prescribed. Finally, the flame shape $f_0(y)$ can be obtained from the kinematic equation

$$f_0'^2 = \left(\frac{S_{Lo}(y^*) + u(y) - u(y^*)}{S_{Lo}(y)}\right)^2 - 1, \tag{10}$$

which implies that the curvature at the leading edge is given by

$$f_0''(y^*) = \sqrt{\frac{u''(y^*) - S_{\mathrm{Lo}}''(y^*)}{S_{\mathrm{Lo}}(y^*)}}\,. \tag{11}$$

Thus, once the flow is specified, all terms in (8) can be determined. For example, in the absence of flow, $u = 0$, y^* is determined simply as the unique maximum of $S_{\mathrm{Lo}}(y)$ which is given by

$$y^* = \frac{S-1}{(S+1)}\left(1 + \frac{|S-1|}{S+1}\right). \tag{12}$$

Then, (8) implies that

$$V \sim S_{\mathrm{Lo}}(y^*) - \left(1 + \frac{l_{\mathrm{F}}}{S+1} + \frac{S\,l_{\mathrm{O}}}{S+1}\right)\epsilon f_0''(y^*), \tag{13}$$

where

$$S_{\mathrm{Lo}}(y^*) = \frac{2^{1/2}\,(S+1)^{1/2}}{S+1-|S-1|}\exp\left(-\frac{1}{2}\frac{|S-1|}{S+1}\right), \tag{14}$$

and

$$f_0''(y^*) = \frac{S+1}{(S+1+|S-1|)\sqrt{2}}, \tag{15}$$

on using (9) and (11).

Applying these results also to the underlying Poiseuille flow (5), we first note that in the flame front region $y \sim 1$ we have

$$u \sim \frac{4S}{(1+S)^2}\,A \tag{16}$$

in the limit $\beta \to \infty$. Thus the flow appears as uniform, with an effective amplitude depending on the stoichiometric coefficient S. This uniformity of the flow for $y \sim 1$ implies that the flame's local burning speed, its leading edge, and its curvature are exactly as is the zero-flow case, described above. The flame speed V, however, depends of course on the flow (5) as dictated by (8) which takes the form

$$V \sim S_{\mathrm{Lo}}(y^*) - \frac{4S}{(1+S)^2}\,A - \left(1 + \frac{l_{\mathrm{F}}}{S+1} + \frac{S\,l_{\mathrm{O}}}{S+1}\right)\epsilon f_0''(y^*) \tag{17}$$

with y^*, $S_{\mathrm{Lo}}(y^*)$ and $f_0''(y^*)$ given by the zero-flow relations (12), (14) and (15). In the particular case $S = 1$, which is the main case to be considered numerically, (17) yields

$$V \sim 1 - A - \left(1 + \frac{l_{\mathrm{F}} + l_{\mathrm{O}}}{2}\right)\frac{\epsilon}{\sqrt{2}}. \tag{18}$$

Finally, we close this section by introducing the propagation speed

$$U \equiv V + u(y^*), \tag{19}$$

which represents the flame speed with respect to the gas located at $y = y^*$, and is thus equal to $S_L(y^*)$, the burning velocity at the leading edge. We note that the sign of U determines whether the flame front is an ignition front ($U > 0$) or an extinction front ($U < 0$). Of course, the asymptotic analysis ϵ cannot reveal extinction fronts since these do not occur for small values of ϵ given that $U \sim S_{\mathrm{Lo}}(y^*)$ is then positive as can be seen from (14). Thus one of the aims of our numerical study is to determine the influence of the flow on the domain of existence of extinction fronts which do occur for non-small values of ϵ.

4. Numerical results

4.1. *Numerical approach*

Triple-flame propagation against the Poiseuille flow (5) in a channel with porous walls is studied numerically. The problem consisting of Equations (1)–(3)with the boundary conditions (6)–(7) is solved using the finite element package COMSOL Multiphysics®. The computations are carried out in a rectangular domain whose typical extent in the x-direction is several hundreds times the planar flame thickness, while in the y-direction it is 2β. The domain is discretised into triangular elements using the default quadratic Lagrange shape function. The gridpoints, typically 200,000, are non-uniformly distributed, as illustrated in Figure 2 showing part of the mesh in a particular case. The flame speed V is updated during the simulation so that the flame remains fixed in the computational domain. Various tests are carried out to ensure that the results are grid-independent.

The parameters varied in the calculation are A (the flow amplitude) and ϵ (the non-dimensional flame front thickness). The Zeldovich number β is also varied in some of the computations. Other parameters are assigned fixed values. Unless otherwise stated, the values $\beta = 10$, $\alpha = 0.85$, $S = 1$ and $\mathrm{Le_F} = \mathrm{Le_O} = 1$ are adopted. Of course, one consequence of the choice $\mathrm{Le_F} = \mathrm{Le_O} = 1$ is that a single equation is needed, say the

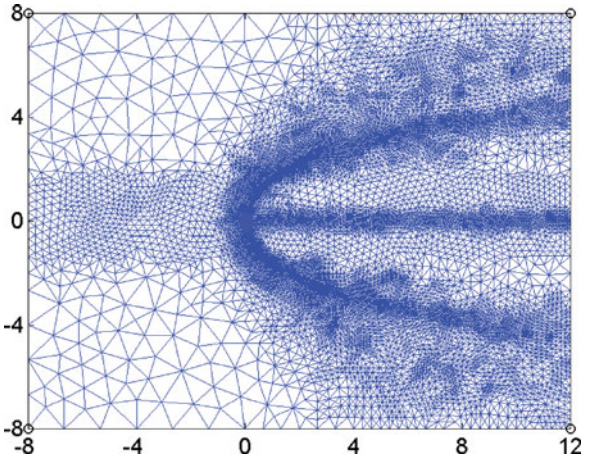

Figure 2. Part of the mesh used in the simulation for $A = -1$. (colour online)

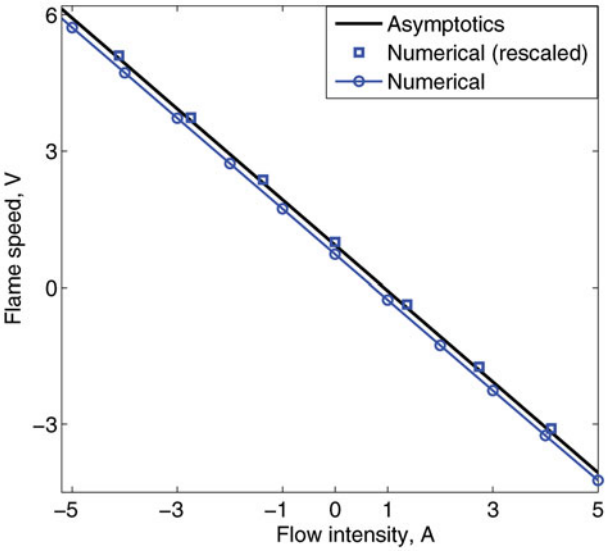

Figure 3. Flame speed V versus A. Comparison between the asymptotic and the numerical predictions for $\epsilon = 0.1$. (colour online)

temperature equation (1), which leads to the reaction rate expression

$$\omega = \frac{\beta^3}{4}\left[1 + \frac{(1+S)y}{2\beta} - \theta\right]\left[1 - \frac{(1+S)y}{2\beta S} - \theta\right]\exp\left[\frac{\beta(\theta-1)}{1+\alpha(\theta-1)}\right].$$

4.2. *Comparison between the asymptotic and numerical results*

To assess the validity of the asymptotic findings summarised in Section 3, and to complement these outside their domain of validity, several sets of calculations are undertaken.

Figure 3 compares the asymptotic prediction of the flame speed V as a function of A (based on formula 18) with the numerical prediction, for $\epsilon = 0.1$. A good qualitative agreement between the asymptotic and the numerical results is seen in the figure, although a small quantitative discrepancy may be observed. This discrepancy is a common problem encountered in triple-flame studies; see for example [7, 12], and is attributed to the finite activation energy ($\beta = 10$) used in the computations while the analytical results are obtained in the asymptotic limit $\beta \to \infty$. The quantitative agreement may be improved by increasing β or, most conveniently, by rescaling both the flame speed V and the flow amplitude A in the numerical results by dividing these by the (numerically computed) laminar flame speed of the stoichiometric planar flame, as done in Figure 3. This type of rescaling has been successfully used in previous studies such as [6, 7, 12]. The quantitative agreement between the asymptotic and the rescaled numerical results in the figure is seen to be excellent.

An additional comparison between the numerical and asymptotic results is given in Figure 4. The figure compares the numerical values of V versus ϵ for $A = 1$, $A = 0$ and $A = -1$ to rescaled asymptotic values.[1] Excellent agreement between the analytical and numerical results is obtained for small values of ϵ (where the asymptotics are expected to be valid), up to values of $\epsilon \approx 0.5$.

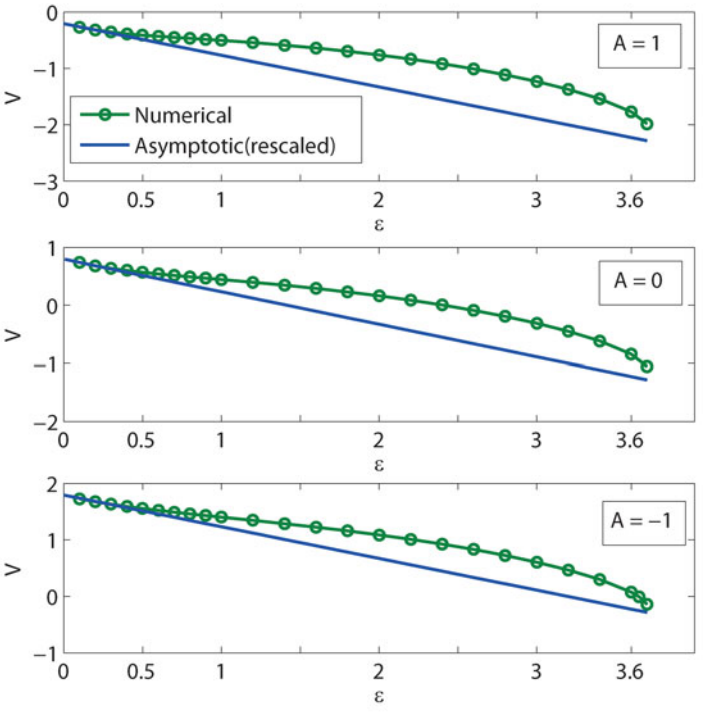

Figure 4. Flame speed V versus ϵ. Comparison between the asymptotic and the numerical results for $A = 1$, $A = 0$ and $A = -1$. (colour online)

4.3. *Effect of the flow amplitude for finite Zeldovich number*

In this section, we describe the effect of varying the flow amplitude A, starting with an illustrative case in Figure 5. Shown are plots of the reaction rate and the temperature for selected values of A, increasing from bottom to top, for $\epsilon = 0.2$. Given in each subfigure is the flame speed V, with $V > 0$ ($V < 0$) indicating that the flame is travelling to the left (right) in the laboratory frame of reference. In the figure, the case $A = 0$ corresponds of course to the usual triple-flame structure consisting of two premixed flame wings and a trailing diffusion flame. In the presence of flow ($A \neq 0$), the triple-flame is observed to retain its usual structure, and only its speed V is affected, as suggested by the asymptotic analysis in [15] summarised in Section 3. We have found indeed that this is the case, except when the flame is opposed by a relatively strong flow, such as for $A = 10$, where the premixed branches are seen to become concave towards the unburnt mixture, and to a lesser extent for $A = 5$, where the change in the concavity of the premixed branches occurs away from the centreline $y = 0$.

This change in the flame structure, which is mainly associated with the non-uniformity of the flow, is not predicted analytically in [15], since in the limit $\beta \to \infty$ adopted there, the flow appears uniform in the flame front region $y \sim 1$, as indicated by Equation (16). In the numerical study, however, as in reality, the (effective) Zeldovich number β is finite, so that the flow non-uniformity must ultimately affect the flame for A larger than a critical value. Although the analytical results may not be able to describe the inversion of flame curvature accurately for finite β, they may be used to provide a qualitative understanding as follows. We first note that in our case, $S = 1$, $u = A - Ay^2/\beta^2$ on using (5), so that the flow

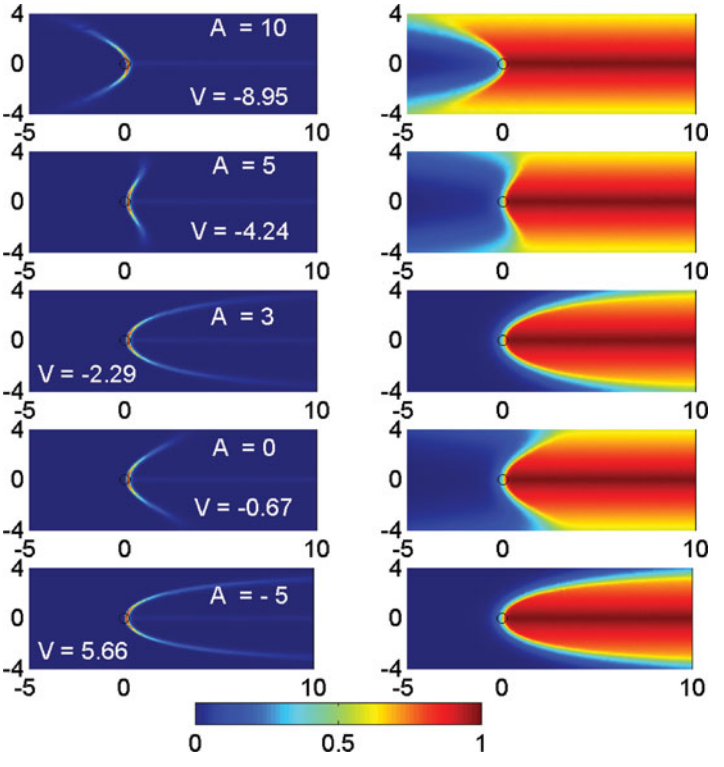

Figure 5. Reaction rate (normalised by its maximum value) and temperature fields for selected values of A and $\epsilon = 0.2$.

non-uniformity is given by Ay^2/β^2. Although this last term vanishes in the distinguished limit $\beta \to \infty$ with $A = \mathcal{O}(1)$ adopted in the analytical study, we shall retain it[2] in the formulas of Section 3 to explain the numerical results for small values of ϵ. Hence, using (9) with $S = 1$, we have

$$S_{\mathrm{Lo}}(y) - u(y) = \sqrt{1 + |y|}\, \exp\left(-\frac{|y|}{2}\right) - A\left(1 - \frac{y^2}{\beta^2}\right),$$

and therefore, for small values of $|y|$,

$$S_{\mathrm{Lo}}(y) - u(y) = 1 - A + \left(\frac{A}{\beta^2} - \frac{1}{4}\right) y^2 + O(|y|^3).$$

This shows that a necessary condition for $y = 0$ to be a leading edge (a maximum of $S_{\mathrm{Lo}}(y) - u(y)$) is that the coefficient of y^2 in the previous equation is negative, i.e. $A < \beta^2/4$. Assuming that this condition holds, permitting the leading edge to be located at the origin, we obtain

$$f_0''(0) = \sqrt{\frac{1}{2} - \frac{2A}{\beta^2}} \qquad \text{and} \qquad U \sim 1 - \epsilon\sqrt{\frac{1}{2} - \frac{2A}{\beta^2}}, \tag{20}$$

on putting $y^* = 0$ in (11) and using (8) and (19).

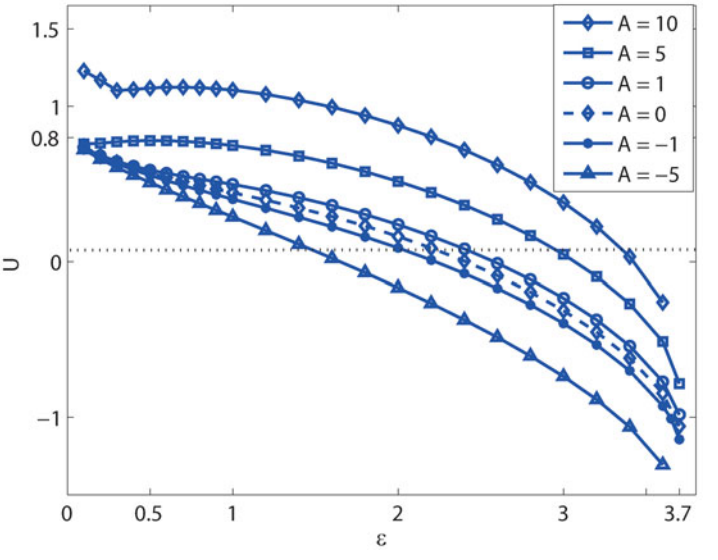

Figure 6. Propagation speed $U = V + A$ versus ϵ for selected values of A. (colour online)

Equation (20) correctly describes the qualitative dependence of the flame front curvature $f_0''(0)$ and the propagation speed U on A, with e.g. U predicted to increase (as can be confirmed from Figures 6 and 7 presented below) and $f_0''(0)$ predicted to decrease with an increase in A. In particular, a change in the flame front concavity is predicted to occur for large *positive* values of A, as observed in Figure 5. The change in the flame front concavity for values of A larger than a critical positive value is due to the kinematic influence of the Poiseuille flow, which tends to make the front concave towards the unburnt gas (for $A > 0$), opposing therefore the influence of concentration gradients. In the context of premixed flames, the kinematic influence of the Poiseuille flow on iso-scalar surfaces and on the

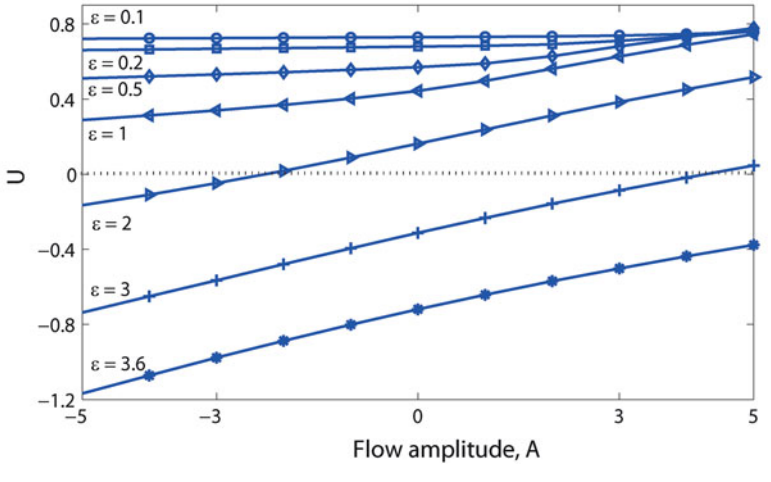

Figure 7. Propagation speed $U = V + A$ versus A for selected values of ϵ. (colour online)

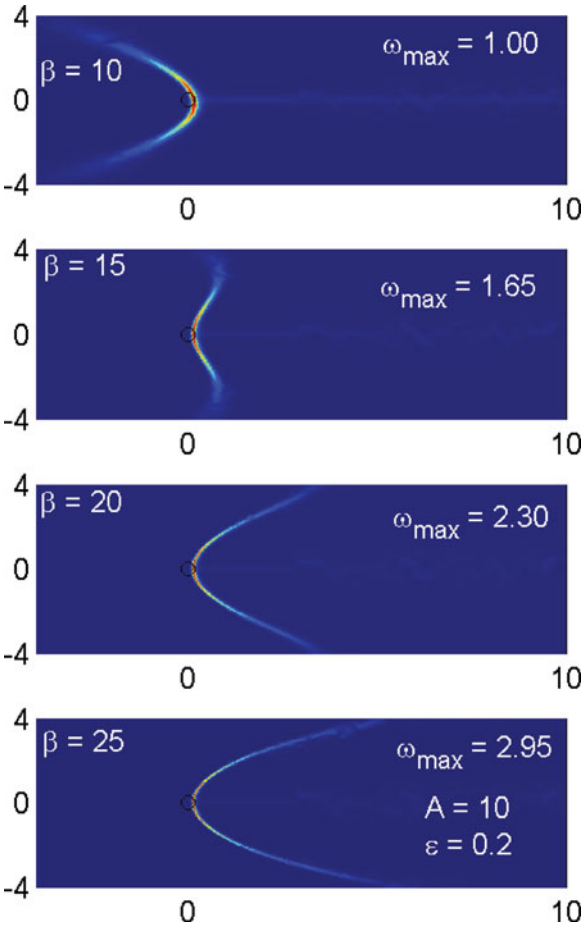

Figure 8. Reaction rate field for selected values of β with $A = 10$ and $\epsilon = 0.2$. (colour online)

propagation speed has been described in [16, 17] for arbitrary positive and negative values of A.

Finally, to confirm further the role of β in the qualitative change in the shape of the triple-flame, we plot in Figure 8 the reaction rate ω for selected values of β when $A = 10$ and $\epsilon = 0.2$. The change in the flame shape from being concave towards the unburnt gas to the ordinary triple-flame shape as β is increased is clearly seen, and can again be understood, qualitatively, from (20).

4.4. *Combined effect of flow amplitude and scale. Ignition and extinction fronts*

To investigate the effect of the flow scale and amplitude on the triple-flame, we plot in Figure 9 the reaction rate ω for selected values of ϵ and A, with $\beta = 10$ fixed here and in the remainder of the paper. Note that ϵ^{-1} provides a non-dimensional measure of the flow scale, since the parameter ϵ defined by (4), measures the flame front thickness relative to (its typical radius of curvature) L/β, and L is the dimensional flow scale. In the figure, the value of ϵ increases from left to right up to near-extinction conditions of the underlying

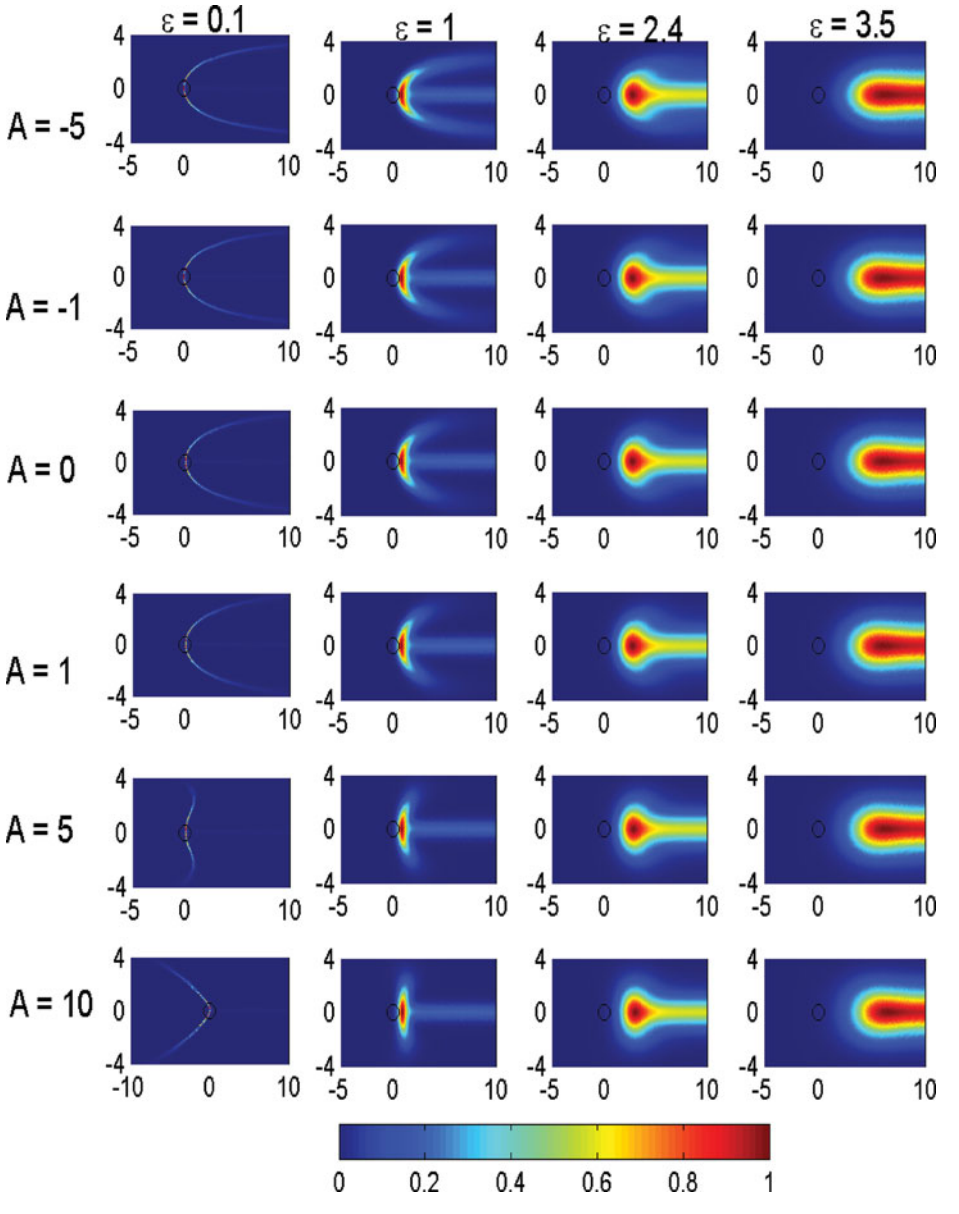

Figure 9. Reaction rate field for selected values of ϵ and A.

diffusion flame, and the values of A increase from negative to positive values from top to bottom. First, we note the major qualitative effect of the flow, namely the change of the front concavity discussed in the previous section, which is found to occur only when ϵ is small and A sufficiently large. Second, we observe that for a given value of A (less than 5 say), the triple-flame shape and behaviour is similar to that encountered in the absence of the flow; as ϵ increases the flame front becomes thicker and its curvature increases which is expected to be accompanied by a decrease in the flame speed. This is confirmed in Figure 10 where the flame speed V is plotted versus ϵ for the same values of A selected in Figure 9.

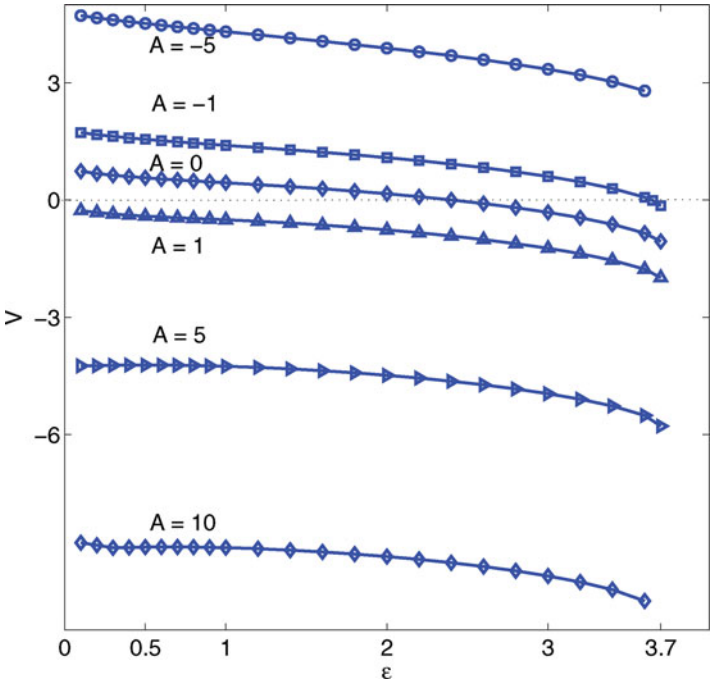

Figure 10. Flame speed V versus ϵ for selected values of A. (colour online)

It is worth reminding the reader that negative (positive) values of V, the flame speed in the negative x-direction with respect to the laboratory, indicate propagation to the right (left), and the numerical value of V is largely determined by the fact the flame is convected by the flow, and all the more so for $|A| \gg 1$. To gain deeper insight into the nature of the flame front, we plot in Figure 6 the quantity $V + A$ versus ϵ. This quantity represents the burning speed $S_L(y)$ (or the flame speed with respect to the unburnt gas) at $y = 0$, namely $S_L(0) = V + u(0)$. The significance of this quantity is due to the fact that the reaction rate of the flame front is strongest at $y = 0$, where the stoichiometric conditions are most favourable, and to the fact that the flame front leading edge y^* is located there, except for sufficiently large values of A such as $A = 10$; see Figure 9. Therefore, $V + A$ typically represents the propagation speed $U \equiv S_L(y^*) = V + u(y^*)$ defined in (19), and its sign determines in all cases whether the flame front (in the vicinity of $y = 0$) is an ignition front ($V + A > 0$) or an extinction front ($V + A < 0$), i.e. whether it is advancing or retreating with respect to the unburnt gas. The figure shows that for thin flames (small ϵ), all curves collapse into a single one if the flow amplitude is not large (all cases with $A < 5$ in the figure); this demonstrates the non-dependence of U on the flow for $\epsilon \ll 1$, as predicted by the asymptotical findings of Section 3. The effect of the flow is more pronounced when ϵ is not small. In particular, it is seen that larger values of A promote combustion by increasing the ϵ-range of existence of ignition fronts, while a decrease in the value of A towards zero or negative values increases the ϵ-range of existence of extinction fronts. This behaviour can be explained by the decrease of the flame front curvature at $y = 0$ with increasing A, which can be observed by careful examination of Figure 9. Finally, we note that the flow has no influence on the maximum value of ϵ at which the flame extinguishes, $\epsilon_{ext} \sim 3.7$, which

corresponds to the extinction of the underlying planar diffusion flame and is obviously unaffected by the presence of a parallel flow.

Similar conclusions to the ones just presented can be drawn from Figure 7, where the propagation speed $U = V + A$ is plotted versus A for selected values of ϵ. The figure also shows that U is a monotonically increasing function of A. This function becomes flat, demonstrating again the non-dependence of U on the flow, in the limit $\epsilon \to 0$ (provided that A is not too large).

4.5. *Effect of flow for stoichiometrically imbalanced mixtures (*$S \neq 1$*)*

The numerical results presented thus far have been restricted to the stoichiometrically-balanced case, $S = 1$, for which the diffusion flame and the leading edge of the triple-flame are located at $y = 0$.

In this section, we examine how non-unit values of S affect the results, by studying numerically the case $S = 2$. This case typifies situations with $S > 1$ for which, in the absence of flow and for small values of ϵ, the leading edge is displaced towards the fuel side, that is $y^* > 0$ as dictated by (12), and the propagation speed $U \sim S_{\mathrm{Lo}}(y^*)$ is determined by (14). Of course, conclusions for cases with $S < 1$ can then be easily inferred, given that if S is changed to S^{-1} ($S \to S^{-1}$), the equations imply that $y^* \to -y^*$ and $U \to U$. Of course, the analysis can be repeated for any value of S.

Shown in Figure 11 are plots of the reaction rate ω for selected values of the flow amplitude A, corresponding to $S = 2$ and $\epsilon = 0.2$. We first observe that, in the absence of flow ($A = 0$), the triple-flame is quite asymmetric, with its leading edge being located above its diffusion tail, which is always situated at $y = 0$ (given the choice of the non-dimensional coordinate y made in Section 2). These observations are in line with those previously reported in the literature, e.g. in [12, 15]. Turning now to the influence of the flow amplitude A, we note that as A is decreased towards negative values, the triple-flame leading edge shifts upwards (towards the fuel side) and that the reaction rate becomes weaker on the upper branch and stronger on the lower branch. The trend is opposite when A is increased towards large positive values, with the reaction rate becoming weaker on the lower-branch and stronger on the upper-branch. Simultaneously, the leading-edge location y^* shifts downwards (towards the oxidiser side), crosses the centreline $y = 0$ (the location of the diffusion flame) for a value of A slightly less than three. For yet larger values of A, slightly larger than four, the lower-branch turns upstream leading effectively to the formation of a premixed flame front with a single branch as seen in the cases with $A = 5$ and $A = 10$. The last behaviour is akin to the change in concavity of the flame front described in the symmetric case $S = 1$ above. As in the latter case, an increase in the value of the Zeldovich number β counteracts the effect of the flow non-uniformity, as illustrated in Figure 12. The figure shows plots of the reactions rate ω for selected values of β when $A = 5$ (left) and $A = -5$ (right). For $A = 5$, it is seen that the triple-flame recovers its usual leading edge and the usual shape of its flame front as β increases. Also, for $A = -5$, an increase in β is seen to weaken the effect of the flow non-uniformity, e.g. by shifting the leading edge back to its position in the absence of flow.

We close this section by attempting to explain the observations just given, in particular the change in the shape of the flame front for sufficiently large positive values of A, by using the analytical formulas of Section 3. The formulas will also explain another fundamental phenomena, namely the appearance of flame-tips where the flame front terminates for $A > 0$; these flame-tips or termination-points are clearly seen in Figure 11 on the lower branch of the flame front in the cases $A = 2$ and $A = 3$. We proceed by putting $S = 2$ in

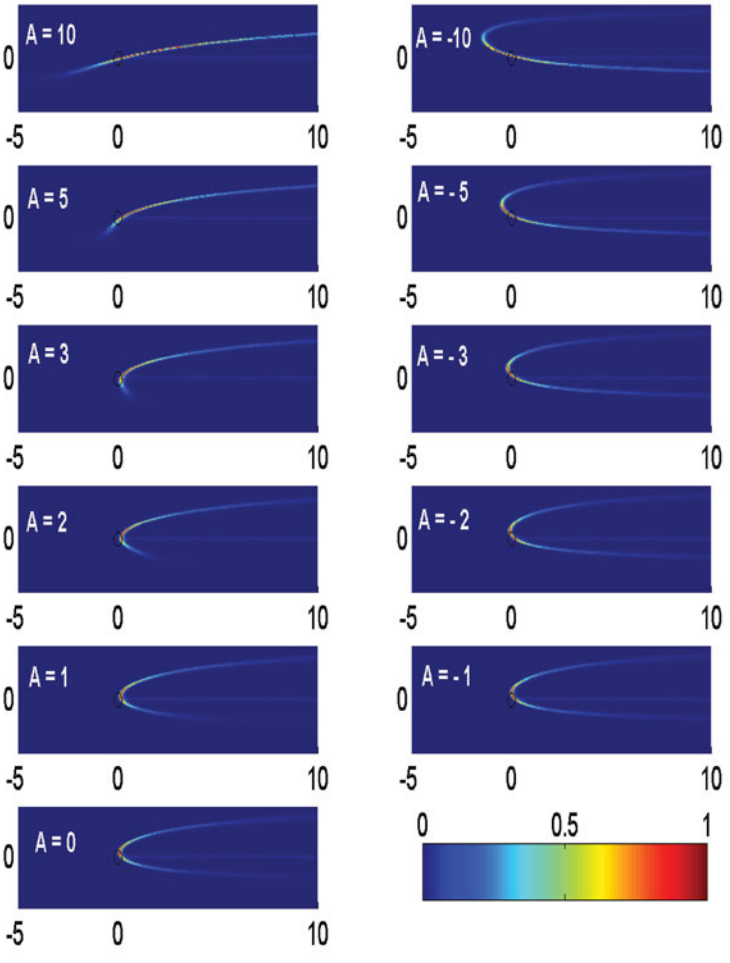

Figure 11. Reaction rate ω for selected values of A when $\epsilon = 0.2$ and $S = 2$.

Equations (5) and (9), to obtain

$$S_{\mathrm{Lo}}(y) - u(y) = \sqrt{1 + \frac{9}{8}|y|}\,\exp\left(\frac{3y - 9|y|}{16}\right) - A\left[1 - \left(\frac{y}{\beta} - \frac{1}{3}\right)^2\right]. \tag{21}$$

The leading edge location y^* is determined as the maximum of the function $S_{\mathrm{Lo}}(y) - u(y)$, and is plotted in Figure 13 versus the flow amplitude A (solid line). The figure shows that such a maximum defining a leading edge may exist only for values of A less than a critical value $A_c = 4.37$, corresponding to the turning point in the figure where the solid line meets the dashed line, the latter being the location of a minimum of the function $S_{\mathrm{Lo}}(y) - u(y)$. The existence of such a critical value explains why the usual flame shape is lost in the numerical results for positive A. The graph also correctly predicts how y^* depends on A as observed in Figure 11; parenthetically we note that (21) implies that $y^* \to 10/3$ as $A \to -\infty$.

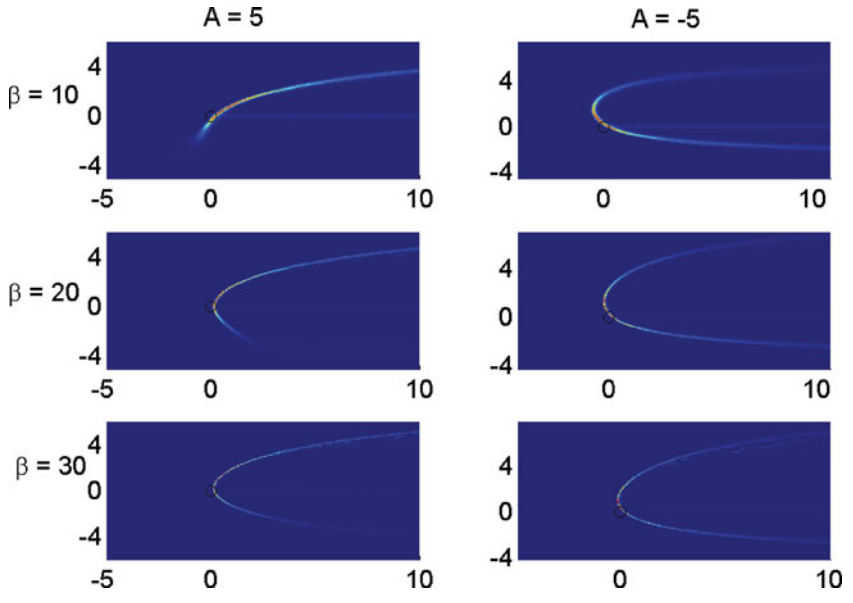

Figure 12. Reaction rate ω for selected values of β when $\epsilon = 0.2$ and $S = 2$. (colour online)

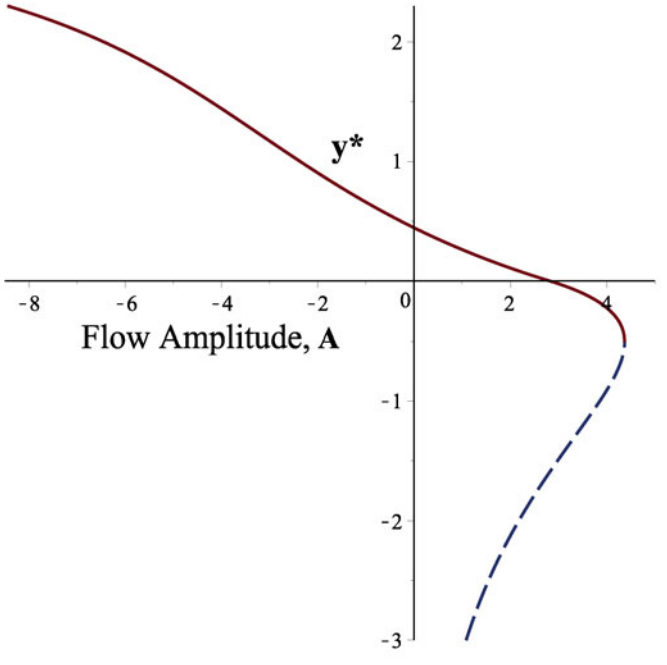

Figure 13. The leading edge location y^* versus the flow amplitude A (solid line) for $S = 2$. The dashed curve corresponds to a minimum of $S_{\mathrm{Lo}}(y) - u(y)$, and the turning point where it meets with the solid line defines the maximum amplitude allowing for a flame edge. The turning point is given by $(A, y^*) = (4.37, -0.510)$. (colour online)

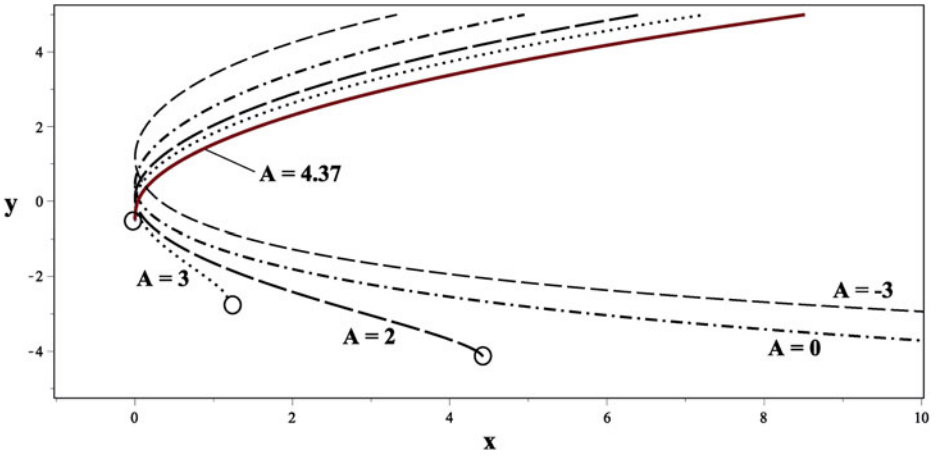

Figure 14. The flame front shape, $x = f_0(y)$ for selected values of A. The circles are flame-tips, or termination-points for the flame front. (colour online)

Finally, to explain the flame shape dependence on A, we turn to the kinematic equation (10), which yields upon integration the curves $x = f_0(y)$ plotted in Figure 14 for selected values of A. The dependence of the flame-shape on A is seen to be in agreement with that already described in Figure 11; note in particular the solid curve corresponding to the critical value $A = A_c = 4.37$ above which no leading edge exists.

An interesting conclusion from the figure is that the flame front does not exist for all values of y in the presence of flow (as is theoretically true when $A = 0$). Rather, there are values of y, negative when $S > 1$ as in the case under consideration, where the flame front terminates. The existence of these termination-points, or flame-tips, can be attributed to the fact that at these points the right-hand side of Equation (10) changes from being positive to negative, which is impossible as the left-hand side, i.e. $f_0'^2$, must be non-negative. Although these termination-points are highly interesting, from both mathematical and physical points of view, we shall not pursue them here any further. Suffice it to say that an analysis similar to that carried out here would reveal that they exist for all values of S, including the symmetric case $S = 1$, if A is larger than a critical positive value depending on S.

5. Conclusion

We have presented a numerical study of triple-flame propagation against a Poiseuille flow in a channel with porous walls, a simple model useful towards understanding the behaviour of a triple-flame opposed by a non-uniform flow. The study tests the findings of a recent analytical investigation [15] obtained for infinitely-large Zeldovich number β and thin flame fronts, $\epsilon \ll 1$. It also extends the description of such flames to situations where the non-dimensional front thickness ϵ and the non-dimensional flow amplitude A are arbitrary, and examines the crucial influence of the finiteness of the non-dimensional activation energy β. Variations in the parameters ϵ, A and β have been considered in this work, as well as in the stoichiometric coefficient S in the last section; other parameters have been assigned fixed values (in particular $\mathrm{Le_F} = \mathrm{Le_O} = 1$).

The numerical study has largely confirmed the validity of the analytical predictions. In particular, it is found that flows of weak or moderate amplitude have a negligible

influence on the flame structure, and that they only modify the flame-front speed V by an amount proportional to A. The numerical study shows however that larger flow intensities can significantly change the flame structure, especially when ϵ is small. More precisely, the concavity of the triple-flame front turns towards the unburnt gas for A larger than a critical value. This behaviour, which cannot be captured by an infinitely-large β asymptotic approach, is found to be intimately linked to the finite values of β which are necessarily found in reality or in any computational investigation. Another new qualitative behaviour which was obtained for small ϵ is the existence of termination-points on the flame front, or flame-tips, seen in Figure 14. These termination-points are shown to exist for $\epsilon \ll 1$ only if A takes on positive values of order unity or larger.

In addition, several novel contributions have been made in the present context of triple-flame interaction with a non-uniform parallel flow. These comprise a description of the flame propagation regimes for a wide range of variations in A and ϵ. In particular, we determine how the flow can promote the existence of ignition or extinction fronts. Specifically, we find that larger values of A promote combustion by increasing the ϵ-range of existence of ignition fronts, while a decrease in the value of A towards zero or negative values increases the ϵ-range of existence of extinction fronts. This behaviour is explained by the decrease of the flame front curvature corresponding to an increase in A. The influence of non-unit values of the stoichiometric coefficient S on the main findings has also been described.

Finally, it should be emphasised that the effect of a non-uniform flow, even one as simple as a parallel flow, on flames propagating in non-uniform reactive mixtures, such as triple-flames, seem to have received few dedicated (theoretical) studies in the literature, despite its potential relevance to practical combustion. We believe that our study is a useful contribution, e.g. in describing the combined influence of the flow amplitude and scale on triple-flame propagation regimes, and in revealing and explaining new behaviour such as triple-flame front inversion and the appearance of flame-tips for suitable values of the parameters A, β and S when $\epsilon \ll 1$. Of course, in order to be able to complete the analytical and numerical studies, and facilitate the understanding of the findings, we have purposely restricted our model by adopting the constant-density approximation. Since variations in density are known to have a major influence on triple-flames [10], the coupling of these effects with the non-uniform flow field considered here, along with the inclusion of other significant effects such as non-unit Lewis numbers and volumetric heat losses, deserve separate investigations. It is hoped that these investigations will include experimental work dedicated to the interaction between simple non-uniform flow fields and triple-flames.

Notes

1. Here we found it convenient to rescale V and A in the asymptotic formula by multiplying them by the (numerically computed) laminar flame speed of the stoichiometric planar flame. Of course, this rescaling (of the asymptotic results) is equivalent to the rescaling of the numerical results in Figure 3.
2. Justification for retaining the non-uniformity term necessitates, strictly speaking, revisiting the analytical work of [15] under a different distinguished limit, such as $\beta \to \infty$ with $A = \mathcal{O}(\beta^2)$, to allow for large values of A. This will not be undertaken here.

References

[1] S.H. Chung, *Stabilization, propagation and instability of tribrachial triple flames*, Proc. Combust. Inst. 31 (2007), pp. 877–892.
[2] H. Phillips, *Flame in a buoyant methane layer*, Proc. Combust. Inst. 10 (1965), pp. 1277–1283.

[3] J. Dold, *Flame propagation in a nonuniform mixture: Analysis of a slowly varying triple flame*, Combust. Flame 76 (1989), pp. 71–88.
[4] K. B. P. Kioni, B. Rogg, and A. Liñán, *Flame spread in laminar mixing layers: The triple flame*, Combust. Flame 95 (1993), pp. 277–290.
[5] J. Hartley and J. Dold, *Flame propagation in a nonuniform mixture: Analysis of a propagating triple-flame*, Combust. Theory Model. 80 (1991), pp. 23–46.
[6] J. Daou and A. Liñán, *The role of unequal diffusivities in ignition and extinction fronts in strained mixing layers*, Combust. Theory Model. 2 (1998), pp. 449–477.
[7] R. Daou, J. Daou, and J. Dold, *The effect of heat loss on flame edges in a non-premixed counterflow within a thermo-diffusive model*, Combust. Theory Model. 8 (2004), pp. 683–699.
[8] J. Daou, R. Daou, and J. Dold, *Effect of volumetric heat loss on triple-flame propagation*, Proc. Combust. Inst. 29 (2002), pp. 1559–1564.
[9] M.S. Cha and P.D. Ronney, *Propagation rates of nonpremixed edge flames*, Combust. Flame 146 (2006), pp. 312–328.
[10] G. Ruetsch, L. Vervisch, and A. Liñán, *Effects of heat release on triple flames*, Phys. Fluids 7(6) (1995), pp. 1447–1454.
[11] Y. Ohki and S. Tsuge, *Flame propagation through a layer with varying equivalence ratio*, Progr. Astronautics & Aeronautics 105 (1986), p. 233.
[12] J. Daou and S. Ali, *Effect of the reversibility of the chemical reaction on triple flames*, Proc. Combust. Inst. 31 (2007), pp. 919–927.
[13] J. Daou, *Asymptotic analysis of flame propagation in weakly-strained mixing layers under a reversible chemical reaction*, Combust. Theory Model. 13 (2009), pp. 189–213.
[14] N.I. Kim, J.I. Seo, Y.T. Guahk, and H.D. Shin, *The propagation of tribrachial flames in a confined channel*, Combust. Flame 146 (2006), pp. 168–179.
[15] J. Daou and F. Al-Malki, *Triple-flame propagation in a parallel flow: An analytical study*, Combust. Theory Model. 14 (2010), pp. 177–202.
[16] J. Daou and M. Matalon, *Flame propagation in Poiseuille flow under adiabatic conditions*, Combust. Flame 124 (2001), pp. 337–349.
[17] J. Daou and P. Sparks, *Flame propagation in a small-scale parallel flow*, Combust. Theory Model. 11 (2007), pp. 697–714.